

The Membrane M Protein Carboxy Terminus Binds to Transmissible Gastroenteritis Coronavirus Core and Contributes to Core Stability

DAVID ESCORS,¹ JAVIER ORTEGO,¹ HUBERT LAUDE,² AND LUIS ENJUANES^{1*}

Department of Molecular and Cell Biology, Centro Nacional de Biotecnología, CSIC, Campus Universidad Autónoma, Cantoblanco, 28049 Madrid, Spain,¹ and Unité de Virologie Immunologie Moléculaires, INRA, 78350 Jouy-en-Josas, France²

Received 31 July 2000/Accepted 7 November 2000

The architecture of transmissible gastroenteritis coronavirus includes three different structural levels, the envelope, an internal core, and the nucleocapsid that is released when the core is disrupted. Starting from purified virions, core structures have been reproducibly isolated as independent entities. The cores were stabilized at basic pH and by the presence of divalent cations, with Mg^{2+} ions more effectively contributing to core stability. Core structures showed high resistance to different concentrations of detergents, reducing agents, and urea and low concentrations of monovalent ions (<200 mM). Cores were composed of the nucleoprotein, RNA, and the C domain of the membrane (M) protein. At high salt concentrations (200 to 300 mM), the M protein was no longer associated with the nucleocapsid, which resulted in destruction of the core structure. A specific ionic interaction between the M protein carboxy terminus and the nucleocapsid was demonstrated using three complementary approaches: (i) a binding assay performed between a collection of M protein amino acid substitution or deletion mutants and purified nucleocapsids that led to the identification of a 16-amino-acid (aa) domain (aa 237 to 252) as being responsible for binding the M protein to the nucleocapsid; (ii) the specific inhibition of this binding by monoclonal antibodies (MAbs) binding to a carboxy-terminal M protein domain close to the indicated peptide but not by MAbs specific for the M protein amino terminus; and (iii) a 26-residue peptide, including the predicted sequence (aa 237 to 252), which specifically inhibited the binding. Direct binding of the M protein to the nucleoprotein was predicted, since degradation of the exposed RNA by RNase treatment did not affect the binding. It is proposed that the M protein is embedded within the virus membrane and that the C region, exposed to the interior face of the virion in a population of these molecules, interacts with the nucleocapsid to which it is anchored, forming the core. Only the C region of the M protein is part of the core.

Transmissible gastroenteritis virus (TGEV) is a member of the *Coronaviridae* family and affects animals, causing severe illness (17, 28). TGEV is an enveloped virus with a single-strand positive-sense RNA genome of 28.5 kb (16; Z. Penzes and L. Enjuanes, submitted for publication), for which an infectious cDNA has been engineered (1). The RNA is bound to the nucleoprotein (N protein), forming a helical nucleocapsid (40). The viral membrane contains three proteins, the spike (S) protein, the membrane (M) protein, and the envelope (E) protein (11, 21, 24, 25). Other coronaviruses also contain an additional membrane glycoprotein, the hemagglutinin esterase (8). The S protein binds to the cellular receptor, the aminopeptidase N (15), and is a determinant of the virus tropism (3, 44). Both the M and E proteins are essential for coronavirus morphogenesis (5, 13, 18, 47). Interactions between these two proteins seem to drive coronavirus envelope assembly, producing virus-like particles in the absence of other viral components. The M protein also binds to the S protein by the amphiphilic domain (14) and to the hemagglutinin esterase, forming homo- and heterocomplexes (37).

An internal core made of RNA and N protein that has

associated with the M protein was recently described (40). The TGEV core was analyzed by different microscopic techniques, such as negative staining, ultrathin sections, freeze fracture, immunogold mapping with monoclonal antibodies (MAbs), and cryoelectron microscopy. The presence of a core in coronaviruses was a novel and unexpected observation. This core appeared to be spherical, but analysis of many electron microscopy preparations of purified cores and platinum-carbon shadowing of the purified cores suggested that it might have an icosahedral shape. The nature, structure, and composition of this core need to be further characterized and studied.

The presence of the M protein in purified cores was somewhat unexpected, since the protein is an integral membrane protein (26, 41, 46). The M protein was part of the cores, since it copurified with them using different gradient conditions, suggesting that a nonspecific interaction was unlikely (40). Given that the M protein is a transmembrane protein, it could specifically bind to the internal nucleoprotein by an intravirion domain forming the core. This last possibility seems feasible because it is known that the M protein interacts with nucleocapsids, at least in mouse hepatitis virus (MHV) virions (46), and this interaction could be responsible for the encapsidation of the viral nucleocapsid into budding virions. This interaction may be mediated by the carboxy-terminal region of the M protein. It was also shown that the M protein interacted with the viral genomic RNA, but it has not been clearly shown

* Corresponding author. Mailing address: Department of Molecular and Cell Biology, Centro Nacional de Biotecnología, CSIC, Campus Universidad Autónoma, Cantoblanco, 28049 Madrid, Spain. Phone: 34-91-585 4555. Fax: 34-91-585 4915. E-mail: L.Enjuanes@cnb.uam.es.

TABLE 1. Mutants used in study

Mutant	Virus sense primer (5'-3')	Reverse-sense primer (5'-3')	Mutations	Restriction sites
M254-256	GAGTGC GCAAGCAAAA TTATTACATATGG	TTTTGCTTGC GCACTCA AATTATCAGTTCTTGCC	A254 A256	— ^c
M248-250	GGCAGCAACTGCTAAT TTGAGTGAG	TTAGCAGTTGCTGCCTC TGTTGAGTAATCACC	A248 A250	— ^c
M216	GGACTATCGATTACAC ACTTGTGGC	ATCGATAGTCCTGCTAG GTAATGCAACC	D216	<i>ClaI</i> 645
M144-145	GGACTATCGATTGGTG GTCTTTCAACCCTG	CCAATCGATAGTCCTTC TGTACAAC TGAATGG	I144 D145	<i>ClaI</i> 431
M62	GGTCTATAATATCGATC GTTTTATAACTGTGC	CGATCGATATTATAGAC CAGCTGAAGTTCCAG	S62	<i>ClaI</i> 184
M96-97	GGCCCGTTGTATCGATT CTTACGATTTTAAATGC	CGTAAGAATCGATACA ACGGGCCATAATAGCC	S96 I97	<i>ClaI</i> 286
M144-145-216 ^a			I144 D145 D216	<i>ClaI</i> 431 <i>ClaI</i> 645
M62-96-97 ^b			S62 S96 I97	<i>ClaI</i> 184 <i>ClaI</i> 286

^a Obtained by combination of the M144-145 and M216 mutants by standard cloning techniques.

^b Obtained by combination of the M62 and M96-M97 mutants by standard cloning techniques.

^c —, no restriction endonuclease site was introduced.

whether the M protein interacts directly with the N protein or with the viral genome (46).

We used multiple approaches in this study to further characterize the association of the M protein within the TGEV core structure. Our results demonstrate that the M protein interacts with the viral nucleocapsid to form the TGEV core. Removal of the M protein destroys the core structure. The interaction appears to be ionic in nature and mediated by the COOH terminus of the M protein. Our results provide insight into how the M protein probably functions as a connector for the viral nucleocapsid during the assembly of mature virions.

MATERIALS AND METHODS

Cells and viruses. Swine testis cells (33) were grown as monolayers in Dulbecco modified Eagle's medium supplemented with 10% fetal calf serum. The TGEV PUR46-MAD strain was grown, purified, and titrated as described previously (24).

TGEV core and nucleocapsid purification. Cores were isolated from 200 to 300 µg of purified TGEV by disrupting the virus envelope with NP-40 at a final concentration of 1% in a disruption buffer (DB) (100 mM Tris-HCl-10 mM MgCl₂ [pH 8]), in the presence of protease inhibitors (Complete Inhibitor Cocktail Tablets; Boehringer Mannheim), for 15 to 30 min at room temperature in a final volume of 500 µl. Cores released from TGEV virions were sedimented through a sucrose gradient (15 to 45%) in DB by centrifugation in an SW60 Ti Beckman rotor at 27,000 rpm for 50 min at 4°C. Fractions were collected from the bottom to the top of the gradient, and core-containing fractions were identified by sodium dodecyl sulfate-polyacrylamide gel electrophoresis (SDS-PAGE) and silver staining. Sucrose was removed from core preparations by diluting the collected fractions with cold DB and ultracentrifugation as described above. Core purity was analyzed by electron microscopy and SDS-PAGE.

Nucleocapsids were obtained from 100 µg of purified cores disassembled with 300 mM KCl in DB (final volume, 400 µl), layered over a 22% sucrose cushion in DB, and centrifuged at 27,000 rpm for 50 min at 4°C in an SW60 Ti Beckman rotor. Nucleocapsids were recovered by resuspension in 50 µl of standard bind-

ing (SB) buffer (10 mM HEPES [pH 7.4], 1 mM dithiothreitol, 10 mM MgCl₂, 50 mM NaCl, 10% glycerol, and 0.1 mM EDTA) (23).

Antibodies. The murine MAbs 5B.H1, 9D.B4, 3D.E3, 3B.B3, and 3D.C10 were previously described (20, 24, 41, 45). The specificities of MAb 25.22 (9, 26) and MAb 1A6 (48, 49) have also been described. MAbs 9D.B4, 3B.B3, and 3D.E3 recognize the carboxy terminus of the TGEV M protein, and MAbs 25.22 and 1A6 are specific for the amino terminus. MAbs 3D.C10 and 5B.H1 recognize the TGEV N and S proteins, respectively. Rabbit anti-β-glucuronidase (GUS) antiserum was purchased from 5 Prime→3 Prime, Inc.

Treatment with chemical agents. Routinely, 50 µg of purified cores was incubated for 10 min at room temperature in DB in the presence of increasing concentrations of different chemical agents in a final volume of 200 µl. After each treatment the cores were washed by ultracentrifugation. The M-to-N molar ratio was estimated after KCl, NaCl, guanidine isothiocyanate, Triton X-100, and 2-mercaptoethanol treatments by SDS-PAGE, silver staining (2), and band densitometry using a Gel Documentation System 2000 (Bio-Rad). For Western blot analysis, the proteins were transferred to a nitrocellulose membrane with a Bio-Rad Mini Protean II electroblotting apparatus at 150 mA for 2 h in 25 mM Tris-192 mM glycine buffer (pH 8.3) containing 20% methanol. Membranes were blocked for 1 h with 5% dried milk in Tris-buffered saline (20 mM Tris-HCl [pH 7.5], 150 mM NaCl). The membranes were then incubated with the MAbs specific for the S, N, M, or GUS protein. Bound antibody was detected with horseradish peroxidase-conjugated rabbit anti-mouse or goat anti-rabbit antibodies and the enhanced chemiluminescence detection system (Amersham Pharmacia Biotech).

Electron microscopy. Negative staining was performed by standard techniques described previously (7). Briefly, samples were adsorbed to UV light-activated copper grids for 2 min at room temperature. Grids were washed two times in DB and stained with 2% uranyl acetate for 30 s. Samples were visualized in a JEOL 1200 EXII transmission electron microscope.

Construction of M gene mutants. The M gene was amplified by PCR from a cDNA clone derived from the PUR46-MAD strain of TGEV, using oligonucleotides that introduced flanking *Bam*HI restriction sites at the 5' end (5'-GCCG GATCCAAAATGAAGATTTTGTTAATATTAGC-3') and 3' end (5'-CGCG GATCCATTTAGAAGTTTAGTTATACC-3'). The M gene was then restricted by *Bam*HI and cloned into the pcDNA3 vector (Invitrogen) digested with *Bam*HI downstream of the T7 promoter, leading to plasmid pcDNA3M.

TABLE 2. Deletion mutants obtained from the pcDNA 3M plasmid

Mutant	Reverse-sense primer (5'-3')	Deletion
MΔ253-262	CCGGGCCCTAATTATCAGTTCCTGCCTC	253
MΔ237-262	CCGGGCCCTTATACATAGTAAGCCCATCC	237
MΔ218-262	CCGGGCCCTAGACAATAGTCCTGCTAGG	218
MΔ146-262	CCGGGCCCATCAAGACTTAGTCCTTCTGTACAAC	146

M gene mutants were produced by overlap extension PCR (38), using synthetic oligonucleotides (Table 1) containing the desired nucleotide substitutions and the plasmid pcDNA3M as a template. Briefly, PCR fragments were obtained either with a T7 promoter primer together with each reverse-sense (RS) primer or with an SP6 primer with each virus sense primer. Both products were recombined and amplified by PCR using T7 and SP6 primers. PCR recombination products were digested with *Bam*HI and were directly cloned into pcDNA3 digested with *Bam*HI. Two mutants, M248-250 (R248 to A and D250 to A) and M254-256 (E254 to A and E256 to A), were generated by clustered charged-to-alanine mutagenesis (4). The rest were obtained as intermediates to construct the internal deletion mutants. A mutant gene, M170 (L170 to V), was spontaneously obtained in a PCR. All mutated genes were cloned into the pcDNA3 vector as described above.

To construct the carboxy-terminal deletion mutants, synthetic oligonucleotides were used to introduce stop codons at different positions (nucleotides 763, 709, 649, and 436) of the M gene followed by an *Apa*I restriction sequence. Briefly, M mutant genes were amplified by PCR from the pcDNA3M plasmid using each of the primers described (Table 2) together with a T7 promoter primer. PCR products were digested with *Bam*HI and *Apa*I and were cloned into pcDNA3 restricted with *Bam*HI and *Apa*I. Four deletion mutants were obtained, MΔ253-262, MΔ237-262, MΔ218-262, and MΔ146-262. In all cases the deletions include the two flanking numbered amino acids. These deletions encode proteins lacking the last 10, 26, 45, and 117 amino acids, respectively.

Two internal deletions were produced by removing the regions encoding the amphiphilic domain (mutant MΔ145-215) and the first and second transmembrane domains (mutant MΔ63-96). To construct mutant MΔ145-215, an intermediate plasmid encoding the M144-145-216 mutant gene (K144 to I, S145 to D, and V216 to D) was produced containing two in-frame *Cla*I restriction sites flanking the sequence encoding the amphiphilic domain. The plasmid pcDNA3M144-145-216 was digested with *Cla*I and religated to obtain the deletion mutant. The MΔ63-96 mutant was obtained using the same strategy by constructing the intermediate pcDNA3M62-96-97 plasmid (L62 to S, L96 to S, and A97 to I). This mutant gene contained the in-frame *Cla*I restriction sites flanking the sequence encoding the first and second transmembrane domains (27).

In vitro-coupled transcription-translation. In vitro-coupled transcription-translation was performed with T7 RNA polymerase in a rabbit reticulocyte lysate (TNT T7 Quick Coupled Transcription/Translation System, Promega) in the presence of [³⁵S]methionine/cysteine (Pro-mix L-[³⁵S]) in vitro cell labeling mix; Amersham Pharmacia Biotech), according to the manufacturer's instructions. Translated proteins were detected by SDS-PAGE and autoradiography. When indicated, unlabeled protein was synthesized by adding methionine to a final concentration of 40 μM. Luciferase and GUS were also produced by using plasmids containing these genes under the T7 promoter. Unlabeled M protein, luciferase, and GUS were detected by Western blotting (results not shown).

Binding assay. The nucleoprotein-specific MAb 3D.C10 (5 to 10 μg) was conjugated to protein G-Sepharose beads (15 μl of Protein G Sepharose 4 Fast Flow; Pharmacia) for 1 h at 4°C in SB buffer to a final volume of 1.5 ml. The beads were collected and washed three times in SB buffer and were incubated with purified nucleocapsids (20 μg/ml, final concentration). The protein G-Sepharose-MAb-nucleocapsid complexes were formed for 4 h at 4°C and were washed three times with SB buffer. Protein G-Sepharose-MAb-nucleocapsid complexes were incubated in the presence or absence of RNase A (60 μg/ml) for 1 h at 37°C. These complexes were used to bind in vitro-translated ³⁵S-labeled wild-type and M mutant proteins (30,000 cpm) by overnight incubation at 4°C. The complexes were washed four times with SB buffer and were dissociated by boiling in SDS-PAGE loading buffer. The bound proteins were resolved by SDS-PAGE, fixed with 10% acetic acid and 5% methanol, and incubated with 14% (wt/wt) sodium salicylate (Merck) for 30 min at room temperature. The gels were dried and exposed to an X-OMAT Kodak Scientific Imaging film at -80°C. In vitro-synthesized ³⁵S-labeled luciferase (30,000 cpm) was used as a control to determine the specificity of the binding assay.

The specificity of the binding between the M protein and purified nucleocapsids was determined by inhibiting the binding with increasing concentrations of in vitro-synthesized, unlabeled M protein. The binding assay was carried out as described above. Equivalent amounts of rabbit reticulocyte lysate alone or lysate including unlabeled GUS were used as controls.

Inhibition of binding of the M protein to the nucleocapsid by increasing concentrations of the indicated MAbs was studied by incubating overnight at 4°C in vitro-synthesized M protein with the indicated MAb concentrations. The complexes were analyzed as described previously. Control immunoprecipitations were carried out in the presence of the S protein-specific MAb 5B.H1.

Inhibition of binding of the M protein to the nucleocapsid by the peptide M233-257 (AYYVKSKAAGDYSTEARTDNLSEQEK), containing the M protein binding domain, was performed by incubating the protein G-Sepharose-MAB 3D.C10-nucleocapsid complex for 2 h at 4°C with ³⁵S-labeled M protein (30,000 cpm) in the presence of increasing concentrations of peptide as described above. Two unrelated peptides of similar length were used as controls (control 1, CVNWLAHNVSKDNRO; control 2, DSYTQGRTFETFKPRSTMEC).

Epitope mapping and relative avidity of M-specific MAbs. The peptides recognized by three different M-specific MAbs were identified by immunoprecipitation. The MAbs 9D.B4, 3B.B3, and 3D.E3 were conjugated to protein G-Sepharose beads. The immunocomplexes were used to bind the deletion mutants MΔ253-262, MΔ237-262, MΔ218-262, MΔ146-262, MΔ145-215, and the M216 mutant. Bound proteins were detected by SDS-PAGE and fluorography as described above.

The relative avidity of MAbs 9D.B4, 3B.B3, and 3D.E3 was estimated by radioimmunoassay (RIA) as previously described (45). Briefly, 250 ng of purified TGEV was plated on a 96-well vinyl assay plate (Data Packaging Corporation) per well. Unbound sites were blocked by 5% bovine serum albumin in phosphate-buffered saline buffer overnight at 37°C. Wells were washed twice with washing buffer (0.1% bovine serum albumin-0.1% Tween 20 in phosphate-buffered saline). Starting from saturating amounts of purified 9D.B4, 3B.B3, and 3D.E3 MAbs (1 μg/ml), 10-fold dilutions were produced in washing buffer and were incubated with the plated virus for 1 h at 37°C. Wells were washed three times, and 50,000 cpm of ¹²⁵I-labeled protein A per well was added and incubated for 1 h at 37°C. Wells were washed four times and dried, and bound radioactivity was measured in a gamma counter. GUS-specific antiserum was used as a negative control.

RESULTS

Treatment of TGEV cores with chemical agents. To study whether the M protein specifically interacts with the internal nucleocapsid to form the core, sucrose gradient-purified cores were treated with different chemical agents, some of them with strong caiotropic properties (Fig. 1). The core structures were better preserved (i.e., provided regular core structures in which sharp edges were frequently observed) at high (8 to 8.5) pH than at neutral (7 to 7.5) pH (Fig. 1 and results not shown). Release of the nucleocapsid was not observed at acid pH.

In order to study whether there was a correlation between the presence of the M protein and core stability, the M protein content and core integrity were analyzed by SDS-PAGE and electron microscopy after treatment with monovalent ions (Fig. 2A). The M protein remained attached to the cores over a wide range (0 to 200 mM) of NaCl or KCl concentrations. Through this range of salt treatment, the core remained a closed entity with only minor changes, as determined by negative-staining electron microscopy (Fig. 2A and B). In addi-

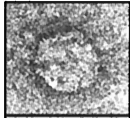
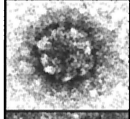
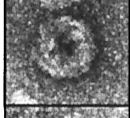
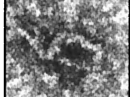
	pH	NaCl mM	KCl mM	Guanidine isothiocyanate, mM	Urea mM	Triton X100 %	2-Mercaptoethanol %
	8-8.5	25-100	25-100	1	10	0.5	0.5-7
	*	*	*	10	25-1000	2 ^a	*
	7-7.5	150-200	150-200	25	*	*	*
	*	300-800	300-800	40-1000	*	*	*

FIG. 1. Effect of chemical agents on virus core structure. Purified cores were treated with different chemical agents using the concentrations indicated in the figure. Representative electron microscopy images of purified cores stained with 2% uranyl acetate after the indicated treatments are shown (left). ^a, the effect of virus core incubation with Triton X-100 concentrations higher than 2% could not be evaluated due to interference with electron microscopy. *, structure not detected after treatment with any concentration of the indicated chemical agent below the maximum value shown within each column.

tion, the protein composition was kept identical to that of the untreated cores. An increase of the salt concentration from 200 to 300 mM led to M protein loss and core disassembly. At monovalent ion concentrations of 300 mM, the core structure was disrupted and the helical nucleocapsid was released. The presence of the N nucleoprotein in the released nucleocapsids was proven by immune electron microscopy with N-specific MAbs (data not shown), as previously described (40). There was an apparent association between M detachment from the cores and disruption of their structure.

In the presence of relatively low concentrations (10 to 25 mM) of guanidine isothiocyanate, the core structure was also affected; for concentrations of this caiotropic agent higher than 40 mM, the M protein was lost and the nucleocapsid was released (Fig. 1 and 2B). Removal of the M protein was linear and directly proportional to the caiotropic agent concentration throughout the whole range of salt concentrations (0 to 100 mM) without an initial plateau (Fig. 2B).

The nonionic detergent Triton X-100 only slightly modified the structure of purified cores up to a concentration of 2%. Incubations for a short period of time (<10 min) in the presence of high concentrations of Triton X-100 did not lead to a change in the core protein composition or to disruption and nucleocapsid release (Fig. 1 and 3A). Triton X-100 concentrations of 2% or higher interfered with electron microscopy (Fig. 3A). Similarly, a reducing agent such as 2-mercaptoethanol in a wide concentration range (0 to 7%) had no apparent effect on the core structure (Fig. 1 and 3B) or the M-to-N molar ratio (Fig. 3B).

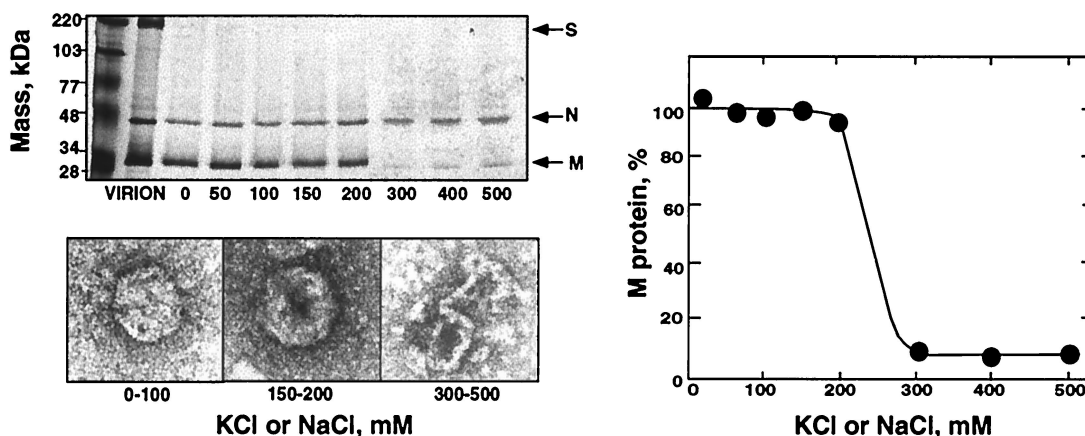
Purified cores were stabilized by the addition of 10 to 25 mM concentrations of divalent cations such as Ca²⁺, Mg²⁺, and Mn²⁺, as determined by negative-staining electron microscopy in comparison with core preparations in the absence of divalent cations (Tris-HCl, 100 mM [pH 8]) (Fig. 4). Chelation of divalent cations by 10 to 25 mM EDTA led to complete core

disruption. When calcium ions were specifically chelated with 10 to 25 mM EGTA, the core structure was partially affected, giving rise to annular-like or strand-like structures.

These results suggest that a domain of the M protein is integrated within the core by ionic interactions and that divalent cations are required to stabilize the core structure.

In vitro binding of ³⁵S-labeled M protein to purified TGEV nucleocapsids. To directly study how M protein may interact with nucleocapsids, a binding assay was established (Fig. 5). A MAb specific for TGEV N protein was conjugated to protein G-Sepharose beads. The conjugated antibody was used to capture purified TGEV nucleocapsids that were then incubated with in vitro-synthesized, ³⁵S-labeled M protein. The wild-type M protein was recovered only when incubated with purified TGEV nucleocapsids (Fig. 5A). Labeled luciferase was used as a control to demonstrate that the nucleocapsid does not bind a nonviral protein (Fig. 5A). The specificity of the binding was further supported by the efficient inhibition of labeled M binding by unlabeled M protein (Fig. 5B). No inhibition was observed when equivalent amounts of reticulocyte lysate alone or lysate including in vitro-synthesized GUS protein were used. These results showed that the M protein-nucleocapsid interaction was saturable and carbohydrate independent, since no glycosylation was introduced by the reticulocyte lysate system that did not include membranes. The M protein was as efficiently precipitated by the nucleoprotein after degradation of the unprotected RNA by RNase as with undigested nucleocapsids (Fig. 5C). The efficiency of the RNase treatment was assessed by the absence of RNA in a standard Northern blot assay, while in the absence of RNase the full-length RNA genome could be observed (not shown). This assay did not exclude the presence of RNA fragments smaller than 100 nucleotides that could have been protected from degradation by the N protein. The N protein that was isolated from the nucleocapsid (RNA plus N protein) in the absence of RNase

A



B

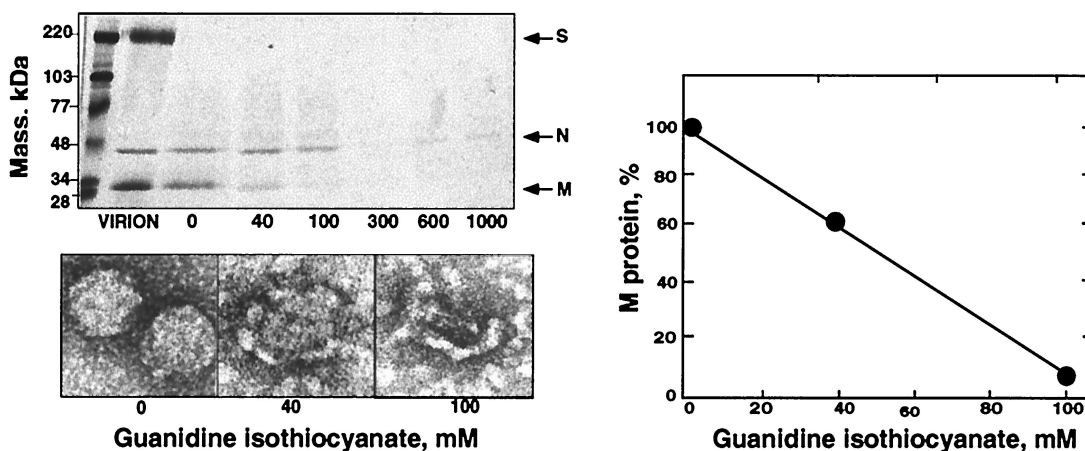


FIG. 2. Treatment of TGEV cores with ionic agents. Purified cores were treated with increasing concentrations of NaCl and KCl (A) or guanidine isothiocyanate (B). For the upper left panels, the protein composition was analyzed by SDS-PAGE using 5 to 20% gradient gels and silver staining. The arrows to the right of the panel indicate the positions of TGEV structural proteins. The core structure observed by electron microscopy after negative staining (2% uranyl acetate) is shown for three representative treatments (bottom left panel). The right panel shows the percentage of the core-associated M protein after each treatment in relation to the M protein of untreated cores. The amount of each viral protein was estimated by densitometry using the N protein as an internal control.

treatment moved to anomalous positions in a bidimensional electrophoresis, while after RNase treatment, most of the N protein was detected in the positions expected for RNA-free N protein (not shown).

Expression of the M protein mutants. In order to further assess the domain of the M protein integrated within the core, a series of deletions were introduced in the M gene, covering selected sequences encoding the potential hydrophilic domains responsible for the interaction with the internal core (Fig. 6). The potential interaction domains are restricted in principle to the C region from amino acid (aa) 134 to the end at aa 262, which is exposed to the cytoplasm in infected cells and to the interior face of the virion membrane (41). Four deletions of increasing size were introduced in the half-M protein carboxy

terminus (M Δ 253-262, M Δ 237-262, M Δ 218-262, and M Δ 146-262; the amino acids with the indicated positions are included in the deletion) (Fig. 6B). In addition, two M protein internal deletion mutants were constructed, one in the region encoding the first and second transmembrane domains (M Δ 63-96) and another one removing a large portion of the internal amphiphilic domain spanning aa 145 to 215 (M Δ 145-215). All M mutant genes were abundantly expressed in a rabbit reticulocyte lysate in the presence of [³⁵S]methionine/cysteine, including those obtained as cloning intermediates (Fig. 6C). The translated proteins showed the expected sizes except one mutant, M254-256, which produced a smaller M protein. The sequence of this mutant was in principle correct, but the alanine codons selected in the construction of this mutant were not the most

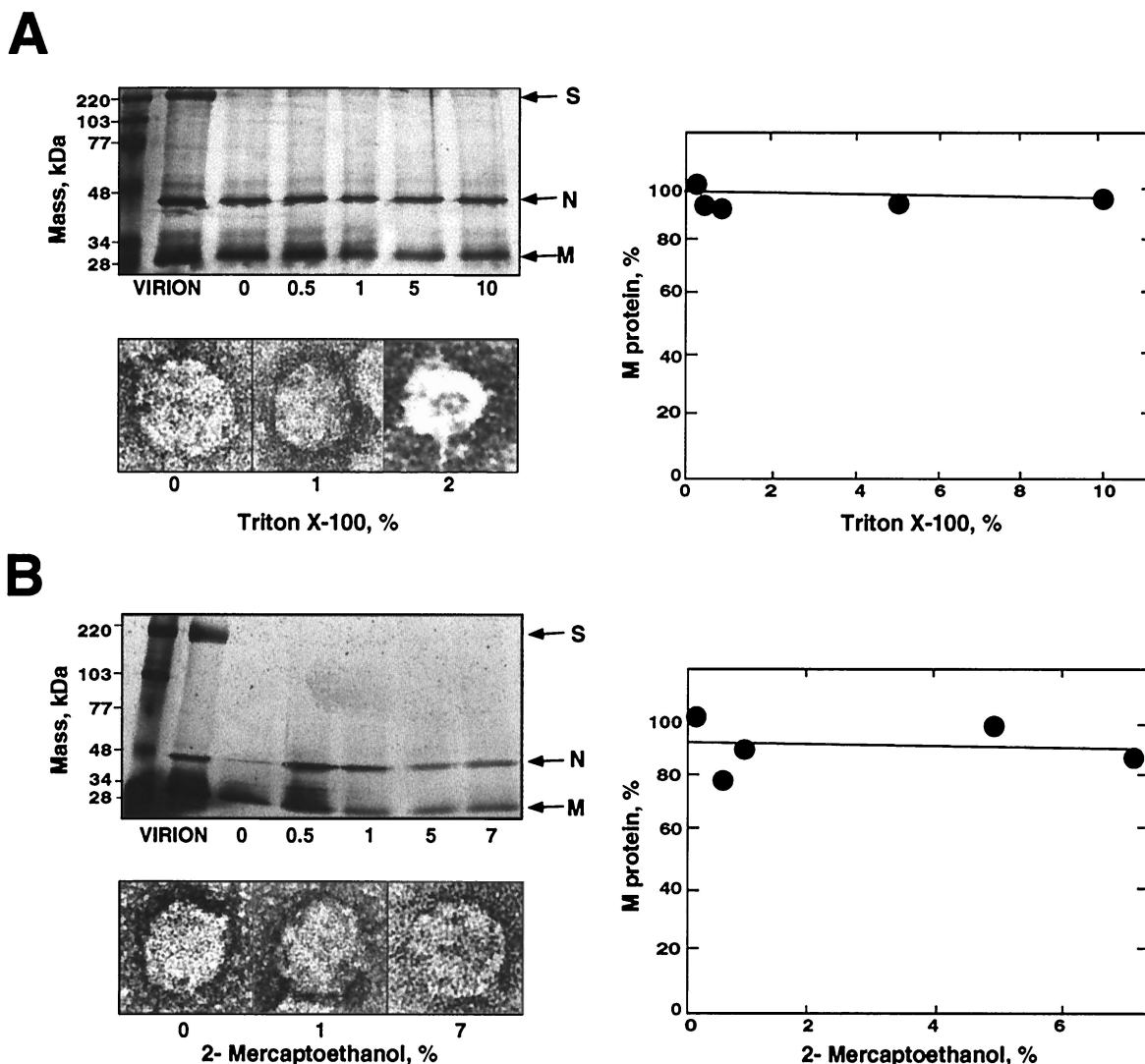


FIG. 3. Treatment of TGEV cores with nonionic agents. Purified cores were treated with increasing concentrations of a nonionic detergent, Triton X-100 (A) or 2-mercaptoethanol (B). The upper left panel shows that the protein composition was analyzed by SDS-PAGE using 5 to 20% gradient gels and silver staining. The positions of the TGEV structural proteins are indicated (arrows to the right of panel). The core structure is shown by electron microscopy of negatively stained specimens (2% uranyl acetate) after three representative treatments (bottom left). The percentage of the core-associated M protein after each treatment in relation to the M protein of untreated cores is also shown (right panel). The amount of virus protein was estimated by densitometry using the N protein as an internal control. The effect of detergent on core structure could not be evaluated when concentrations of Triton X-100 higher than 2% were used, due to interference with electron microscopy.

frequently used in eukaryotic cells, probably causing a stop in the translation at residue 253 (GCG codon in the 760 position, in contrast to GCT codons for other alanine substitutions).

Two bands were observed for all the in vitro-synthesized M proteins. One of these bands presented the expected size, while the other had a reduced one. The smaller M protein probably corresponds to internal in vitro initiations of M protein synthesis.

Epitope mapping and relative avidity of M protein-specific MAbs. The M protein domain recognized by three MAbs (9D.B4, 3D.E3, and 3B.B3) (45) was previously located at its carboxy terminus (20, 24, 41, 45). The discrete domains recognized by each of these three M-specific MAbs were differentiated by immunoprecipitation using the M protein deletion mutants described above (Fig. 6). MAb 9D.B4 immunoprecipi-

tated the deleted M proteins MΔ253-262, MΔ237-262, and MΔ218-262 but not MΔ146-262 (Fig. 7) or MΔ145-215 (not shown), strongly suggesting that an epitope comprised within M protein aa 146 to 217 was recognized by this MAb. Interestingly, a mutation of leucine 216 to glutamine (M216) abolished M protein recognition by MAb 9D.B4, indicating that an epitope that includes this amino acid was recognized by MAb 9D.B4. Both MAbs 3D.E3 and 3B.B3 efficiently immunoprecipitated the wild-type M protein, the M216 mutant, and the MΔ145-215 (not shown) but not the deletion mutants (MΔ253-262, MΔ237-262, MΔ218-262, and MΔ146-262) (Fig. 7). This result indicates that the peptides recognized by these antibodies mapped in the last 10 residues.

The relative avidity of MAb 3D.E3 for the M protein was

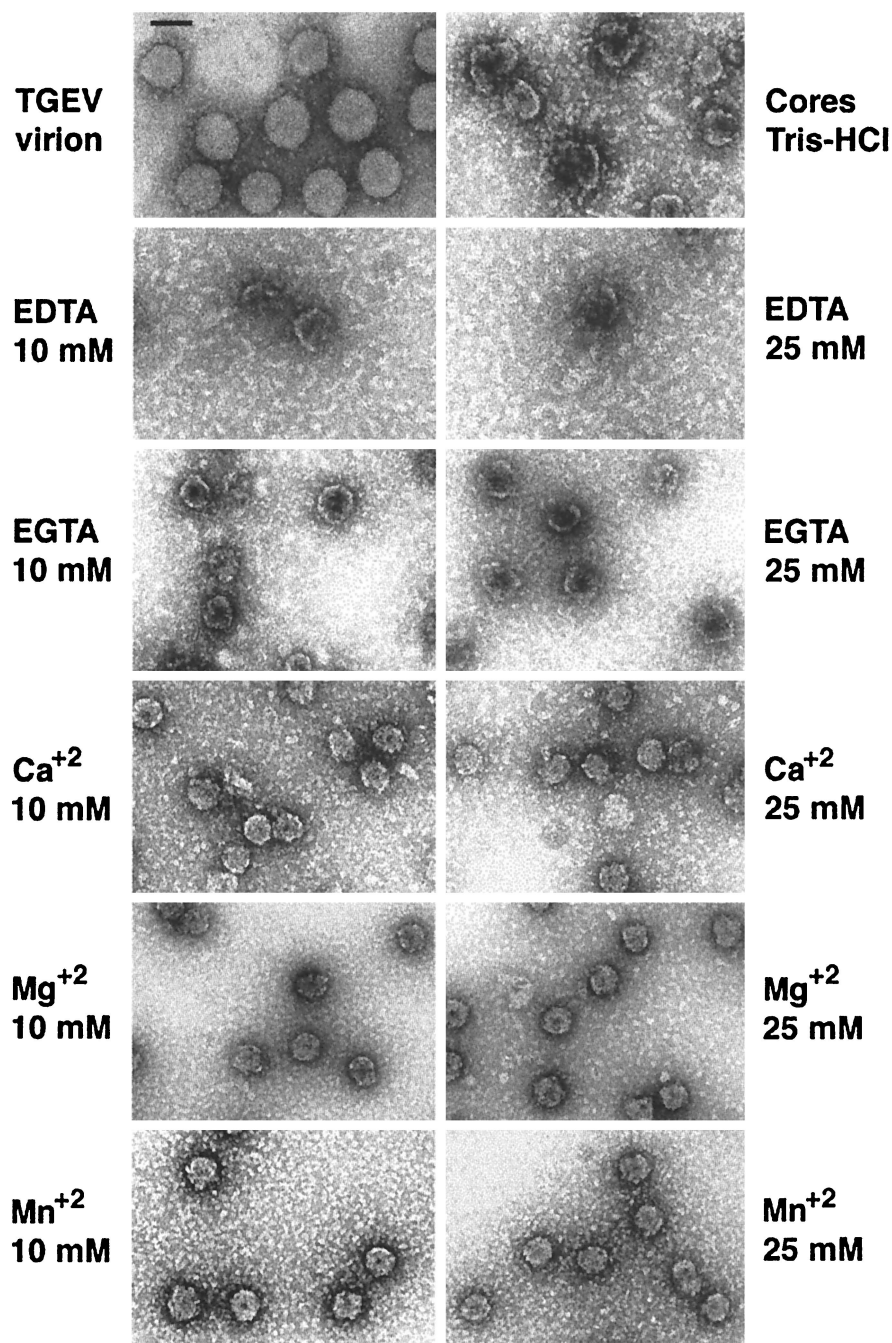


FIG. 4. Effect of divalent cations on the core structure. Representative electron micrographs of purified TGEV virions stained with 2% uranyl acetate are shown (topmost left). The rest of the panels show electron microscopy images of cores incubated in 100 mM Tris-HCl (pH 8) for 15 min at room temperature in the presence of cation chelating agents (EDTA or EGTA) or divalent cations. Bar, 100 nm.

higher than that of MAb 3B.B3 and 9D.B4, as determined by RIA and immunoprecipitation (Fig. 8). In fact, the binding in RIA of identical amounts of purified MAb 3D.E3, 3B.B3, and 9D.B4 to TGEV showed a higher plateau for MAb 3D.E3 than for MAb 3B.B3 and 9D.B4, even when a larger excess of the antibodies was added (Fig. 8A). MAb 9D.B4 also presented a higher avidity than did 3B.B3. In addition, a higher binding level was reproducibly shown for MAb 3D.E3 over 9D.B4 and 3B.B3 by immunoprecipitation analysis (Fig. 8B). Since MAb

3D.E3 and 3B.B3 bind to the same 10-residue peptide, they will possibly recognize partially overlapping epitopes.

MAb 25.22, previously characterized as a MAb binding the M protein amino terminus (9, 26), and MAb 1A6 (48, 49), also specific for the M protein amino terminus, bound all deletion mutants portrayed in Fig. 6 (data not shown), confirming that these MAb were directed to the amino-terminal domain.

Inhibition of binding of the M protein to nucleocapsids by M-specific MAb. In order to identify the domain of the M

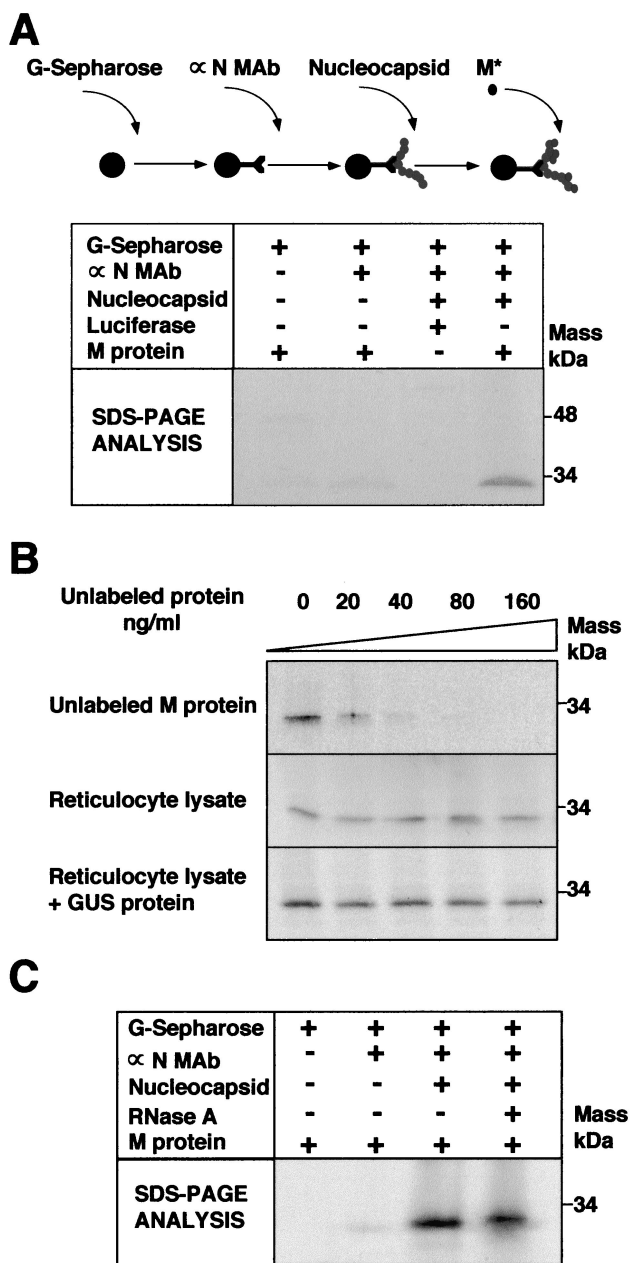


FIG. 5. Interaction of ³⁵S-labeled M protein with purified nucleocapsids. (A) Scheme of the assay developed to study the binding of the M protein to a nucleocapsid based on protein G-Sepharose beads coated with MAb 3D.C10 specific for the N protein (α N MAb) and purified nucleocapsids (top). Wild-type M protein and luciferase were transcribed in vitro and labeled with [³⁵S]methionine/cysteine. M protein or luciferase was incubated with the nucleocapsid complex, and the bound proteins were analyzed by SDS-PAGE and fluorography (lower part of panel A). + and -, presence and absence of the indicated component in the assay. (B) Inhibition of binding of the M protein to a nucleocapsid by increasing concentrations of unlabeled proteins. The bound M protein was analyzed by SDS-PAGE and fluorography. (C) Effect of nucleocapsid immunocomplexes' incubation with RNase (60 μ g/ml for 60 min at 37°C) on recognition of the M protein in the assay described for panel A.

protein involved in the binding of this protein to the nucleocapsid, inhibition of this interaction by the M-specific MABs was studied. MABs 9D.B4 and 3D.E3 significantly inhibited the binding of the M protein to the nucleocapsid, but MAB 3B.B3 showed a reduction of this binding that was statistically non-significant (Fig. 9). In contrast, MABs 25.22 (9, 26) and 1A6 (48, 49), specific for the M protein amino terminus, or excess MAB 5B.H1, specific for the S protein (20), did not inhibit the binding. These results indicate that the binding of the M protein to the nucleocapsid was specific and that it was mediated by the carboxy terminus of the M protein. MAB 3D.E3 strongly inhibited the interaction even at low antibody concentrations (4 μ g/ml), while MAB 9D.B4 required around a 10-fold-higher concentration to inhibit the binding to the same extent, suggesting that MAB 3D.E3 was bound to the M protein in a domain closer to the N protein binding site. Alternatively, this MAB has a higher avidity for the M protein than does MAB 9D.B4 or a combination of both. Interestingly, a correlation between relative avidity for the M protein and inhibitory activity was observed (Fig. 8 and 9).

The two M protein bands expressed in vitro, which can often be resolved in the SDS-PAGE analysis, were bound to the N protein (results not shown).

Binding of ³⁵S-labeled M protein mutants to the TGEV nucleocapsid. To more precisely define the M protein domain involved in binding to the nucleocapsid, the binding of all the constructed M protein mutants (Fig. 6) to the TGEV nucleocapsid was assayed as described above (Fig. 5). The most significant results are shown (Fig. 10). Substitution of a few amino acids throughout the M protein did not affect its interaction with the nucleocapsid. A deletion covering the first and second transmembrane domains, including the short intraviral hydrophilic portion (from residues 70 to 80) did not prevent the interaction, in addition to a deletion from residue 253 to the carboxy-terminal end of the M protein. However, deletions from residue 237 to the carboxy-terminal end completely abolished interaction of the M protein with the viral nucleocapsid. None of the other M protein mutants with a larger deletion, including from residue 237 to the end, were bound to the nucleocapsid, as could be expected (data not shown). Interestingly, the removal of residues 145 to 215, covering most of the intraviral domain of the M protein, had no effect on the interaction. All these results strongly suggest that the M protein specifically interacts with the viral nucleocapsid through residues located from aa 237 to 252 (Fig. 10). Interestingly, this interaction domain corresponds to the most hydrophilic region of the carboxy-terminal end.

Inhibition of binding of the M protein to the nucleocapsid by a synthetic peptide. To confirm that the residues between positions 237 and 252 correspond to the interaction domain, inhibition of binding of the wild-type M protein to the nucleocapsid by increasing concentrations of a synthetic peptide, M233-257 (including aa 237 to 252 of the M protein) was studied (Fig. 11). Binding of the M protein to the nucleocapsid was completely inhibited by the peptide M233-257 at a concentration of 40 μ M. No binding inhibition was observed when short (C1) or long (C2) unrelated peptides were used, confirming the specificity of the inhibition.

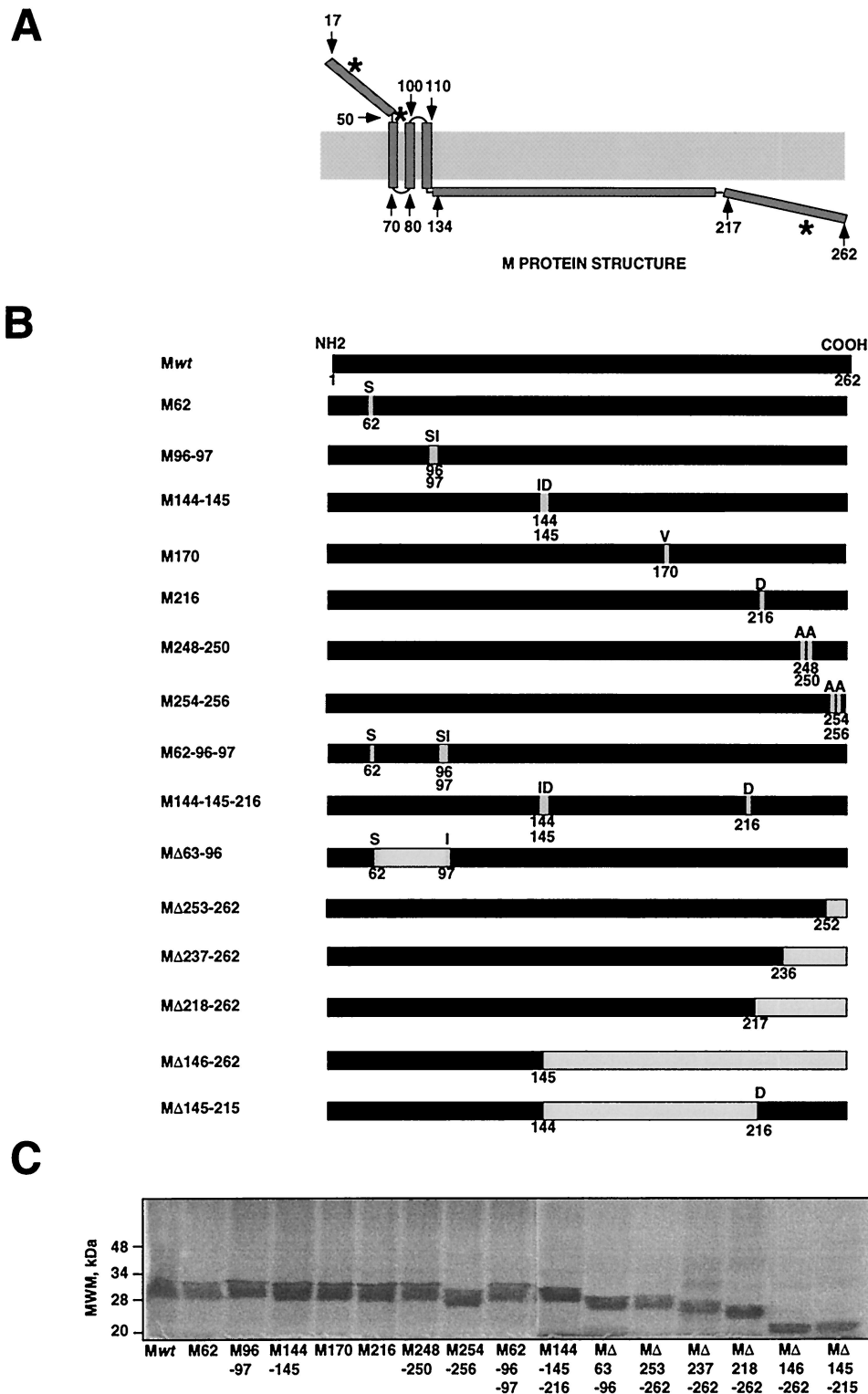


FIG. 6. Generation of M gene mutants by site-directed mutagenesis. (A) Model of M protein topology with amino terminus-exo carboxy terminus-endo topology in the virion membrane. Predicted glycosylation sites are indicated by asterisks. Numbered arrows indicate the amino acid positions in the model. (B) Scheme of the M protein mutants generated. Numbers below the bars indicate the mutated amino acid (substitution mutants) or flanking amino acids in the deletion mutants. The mutated amino acid or the flanking amino acids of each deletion are indicated above the bars. Substitutions or deletions are indicated by open boxes within bars. Mutant names are indicated in the left column. (C) The mutant genes were expressed in a rabbit reticulocyte lysate in the presence of [³⁵S]methionine/cysteine and were analyzed by SDS-PAGE and autoradiography.

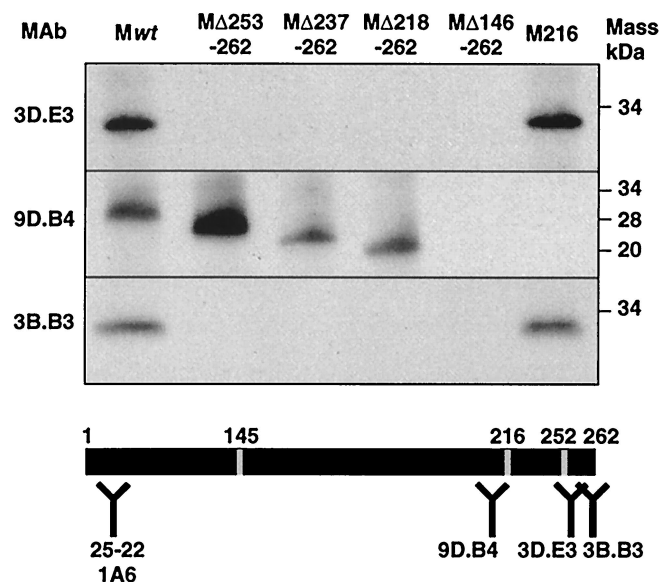


FIG. 7. Mapping of the domains recognized by the M protein-specific MAbs. Carboxy-terminal deletion mutants were expressed in a rabbit reticulocyte lysate in the presence of [³⁵S]methionine/cysteine and were immunoprecipitated with M-specific MAbs. The immunoprecipitated proteins were analyzed by SDS-PAGE and fluorography. The M protein domains recognized by the MAbs used are indicated within the bar. Numbers on the top of the bar indicate amino acid positions.

DISCUSSION

In this work it has been shown that the C domain of the M protein is an integral part of cores that can be purified from TGEV virions, since removal of the M protein led to core dissociation. The core structure was stabilized by the presence of divalent cations and high pH and was resistant to nonionic detergents and reducing agents. The domain of the M protein that interacts with the nucleocapsid mapped to residues 237 to 252. Interactions between the M protein and the nucleocapsid were of an ionic nature. Studies on TGEV virion structure by several ultrastructural techniques have shown that the viral nucleocapsid is arranged in a spherical core that can be isolated as an independent entity (40). Studies on TGEV morphogenesis also show that immature TGEV virions contain an annular core structure. Major reorganization of this annular core during viral maturation produces a smaller and geometrical internal core (42, 43).

To eliminate the possibility that the M protein unspecifically collapsed on the core surface, several chemical agents were used to disrupt the M protein-N protein interaction within the core. Treatments with ionic agents at concentrations that did not modify the M-to-N molar ratio within the cores did not disrupt the core structure. Interestingly, at high concentrations of the ionic agents, there was a correlation between loss of the M protein and complete core disassembly, suggesting that the M protein plays an important role in maintaining the core structure. Nevertheless, it is not possible to rule out that the increase in monovalent ion concentration could also affect binding of the N protein to RNA or N protein-homotypic interactions, affecting the overall core stability.

Only minor effects on the core, which maintained its struc-

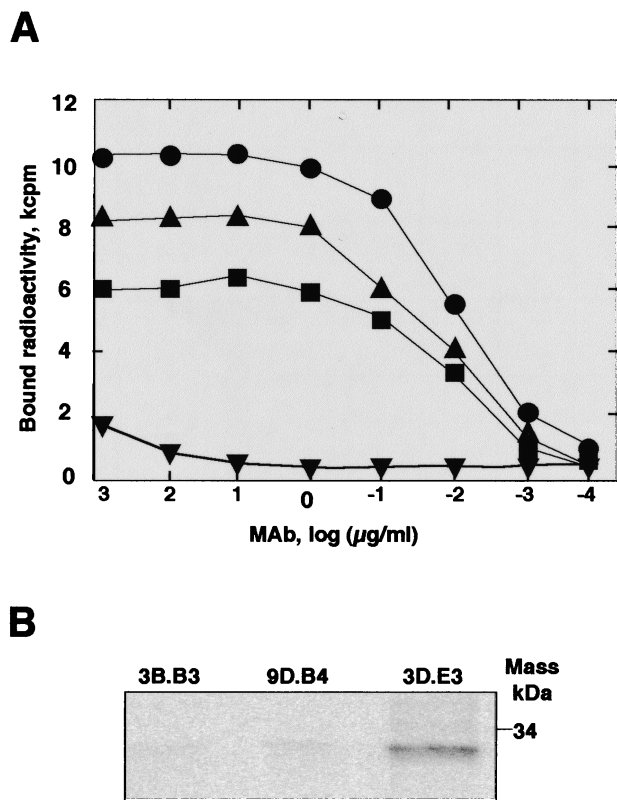


FIG. 8. Relative avidity of M-specific MAbs. (A) Binding of MAbs 3D.E3 (●), 3B.B3 (■), and 9D.B4 (▲) and polyclonal serum rabbit anti-GUS (▼) to the TGEV M protein as determined by RIA to estimate the MAb relative avidity for the M protein. (B) Analysis by SDS-PAGE and autoradiography of the M protein immunoprecipitated by these MAbs.

tural entity, were observed after treatment with Triton X-100 or 2-mercaptoethanol, which did not alter the M-to-N molar ratio within the cores. The M protein remained bound to purified cores even when extremely high concentrations of these agents were used. These results showed that the M protein interaction was not of a hydrophobic nature or dependent on disulfide bonds but was of an ionic nature.

Divalent cations preserved TGEV core structure. This requirement has also been observed for polyomavirus, rotavirus, and plant viruses (turnip crinkle virus) among others (6, 19, 29, 30).

The in vitro-synthesized M protein specifically bound purified nucleocapsids. In fact, four of the M protein deletion mutants bound the nucleocapsid and three did not, suggesting that most likely the structure of the M protein domain involved in the binding is not affected by the deletions unless the deletion removes amino acids directly involved in the interaction. The M protein apparently interacts with the N protein itself but not with the unprotected viral RNA, because digestion of the unprotected RNA had no effect on the binding assay. In addition, when the purified N protein was bound to the Sepharose beads in the absence of viral RNA, no binding of the M protein was observed (results not shown). These results suggest that binding of the N protein to the RNA possibly induces a conformational change in the N protein that facilitates the

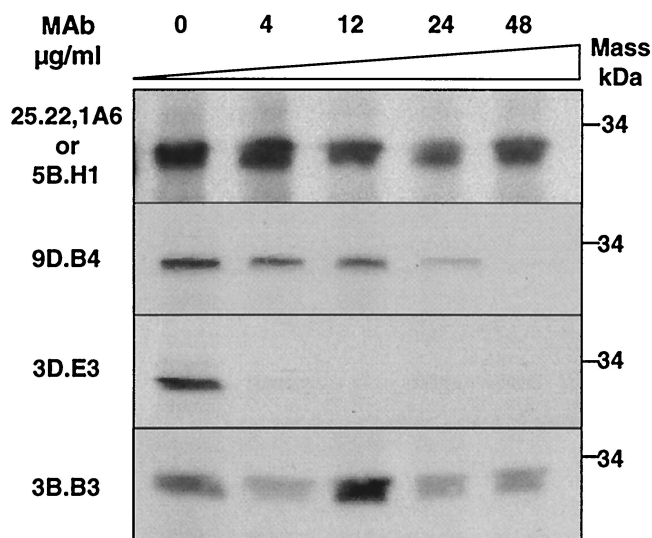


FIG. 9. Inhibition of binding of the M protein to nucleocapsids by M-specific MAbs. Inhibition of binding of the M protein to nucleocapsids by MAbs 9D.B4, 3D.E3, and 3B.B3 (specific for the M protein carboxy-terminal domain) and by MAbs 1A6 and 25.22 (specific for the amino-terminal domain of the M protein) was analyzed as described for Fig. 5. Labeled M protein was incubated with the protein G-Sepharose-MAb 3D.C10 complex coated with the viral nucleocapsid in the presence of increasing concentrations of MAb. Bound M protein was analyzed by SDS-PAGE and fluorography. Control immunoprecipitations were carried out in the presence of the S-specific MAb 5B.H1.

interaction between the N and M proteins. The interaction between these two proteins has also been observed in TGEV-infected swine testis cells (J. Ortego, D. Escors, and L. Enjuanes, data not shown), strongly suggesting that this interaction is not an artifact resulting from *in vitro* assays. In fact, intracellular interaction between the M and the N proteins has also been reported for MHV (36).

According to the topology of the M protein and its hydrophilic pattern (41), the potential interaction domains were restricted to three: a zone located between the first and second transmembrane domains (residues 70 to 80), certain parts of the amphiphilic domain (residues 134 to 217), and most of the carboxy-terminal domain (residues 217 to 262) (Fig. 6A). Three complementary approaches led to the conclusion that this interaction was mediated by a domain of the M protein mapping between amino acids 237 and 252. First, it was shown that two MAbs specific for the carboxy terminus specifically inhibited binding of the M protein to the nucleocapsid, suggesting that the interaction domain was restricted to the carboxy terminus, close to the peptide recognized by MAb 3D.E3. Secondly, the location of the M protein domain interacting with the nucleocapsid was confirmed by binding of M protein deletion mutants to purified nucleocapsids. Only the M protein mutants with a deletion between positions 237 and 252 did not bind the nucleocapsid. Finally, interaction of the M protein with the virus nucleocapsid was inhibited by a synthetic peptide spanning aa 233 and 257. A molar ratio of peptide to ligand of about 10-fold strongly inhibited the binding. This peptide concentration (40 μ M) is below the level (60 μ M) required to inhibit interactions between the envelope glycoproteins and

the matrix or the N protein of Semliki Forest virus and hepatitis B virus, respectively (35, 39). The results shown here indicate that the M protein specifically interacts with the nucleocapsid via the carboxy terminus. This is not uncommon, since viral membrane glycoproteins usually interact either with an internal matrix protein such as in retrovirus (12), rhabdovirus (34), and orthomyxovirus (50) or directly with the core or nucleocapsid (10), as in the case of alphavirus (22, 31, 32, 35).

The TGEV nucleocapsid is arranged in a spherical core. The structure of this seems to be stabilized and maintained by the interaction between the M protein and the nucleocapsid. Therefore, the M protein carboxy terminus would be a structural part of the core, since it was not possible to purify intact TGEV cores lacking the M protein. It has been previously reported (41) that the M protein is present in the TGEV envelope in two topologies, one of them with the carboxy terminus in the virus interior, which is the most abundant, and another one present in a significant proportion with the carboxy terminus facing the virion surface. Recent biochemical data have confirmed the presence of these two M protein topologies within the TGEV envelope (D. Escors, J. Ortego, and L. Enjuanes, unpublished data). According to this model, only the M protein with an NH₂-exo COOH-endo topology

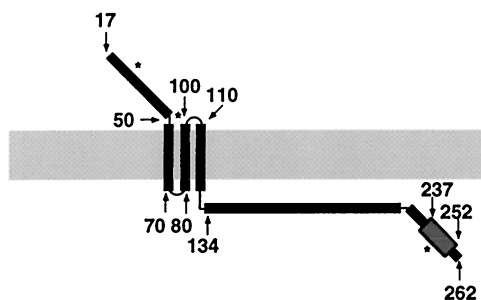
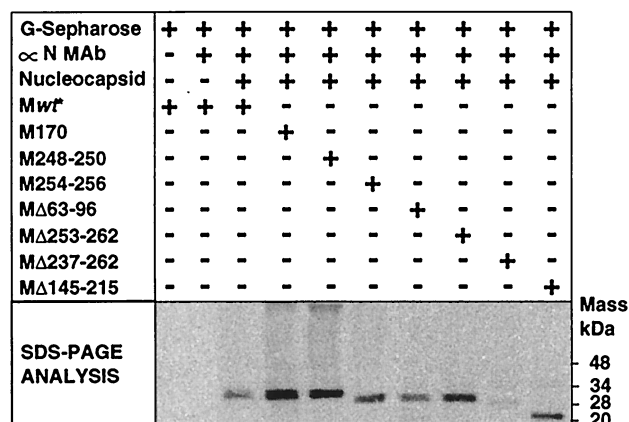


FIG. 10. Binding of M protein mutants to purified nucleocapsids. The binding of ³⁵S-labeled M protein mutants to viral nucleocapsids was performed as indicated for Fig. 5. Bound M protein was analyzed by SDS-PAGE and fluorography. + and -, presence and absence of the component in the reaction mixture. The scheme (bottom) illustrates the topology of the M protein with the conformation amino terminus-exo, carboxy terminus-endo within the virus envelope. Predicted glycosylation sites are indicated by asterisks. Numbered arrows indicate the approximate position of the amino acids in the model. wt, wild type.

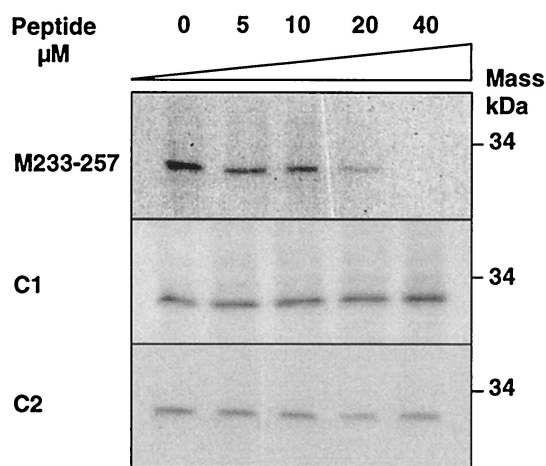
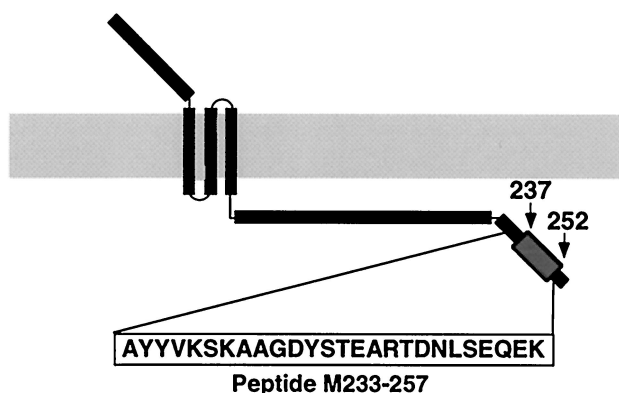


FIG. 11. Inhibition of binding of the M protein to nucleocapsids by using synthetic peptides. The localization of the M233-257 peptide within the M protein is illustrated (top panel). Inhibition of binding of the M protein to nucleocapsids (Fig. 5) by increasing concentrations of the indicated synthetic peptides was analyzed by SDS-PAGE and fluorography.

would interact with the TGEV core, while the M protein with an NH₂-exo COOH-exo topology would potentially be removed during the dissolution of the virus envelope to purify the virus core.

It has also been recently shown (14) that the M protein interacts with the S protein via the amphiphilic domain. Consequently, the M protein is a multifunctional protein with a crucial role in coronavirus assembly. It could interact in the membrane with the S protein and with the E protein. At the same time, its C-terminal domain is integrated within the viral core to drive coronavirus assembly.

ACKNOWLEDGMENTS

We thank Amelia Nieto and Brenda Hogue for critical reviews of the manuscript.

This research was supported by grants from the Comisión Interministerial de Ciencia y Tecnología (CICYT, Spain), the Dirección General de Investigación (Community of Madrid), the European Community (Key Action 2, Control of Infectious Diseases Program), and Fort-Dodge Veterinaria S. A. (Spain). D.E. and J.O. received a fel-

lowship and contract from the Spanish Department of Education and Culture.

REFERENCES

- Almazan, F., J. M. González, Z. Péntez, A. Izeta, E. Calvo, J. Plana-Durán, and L. Enjuanes. 2000. Engineering the largest RNA virus genome as an infectious bacterial artificial chromosome. *Proc. Natl. Acad. Sci. USA* **97**: 5516–5521.
- Ansorge, W. 1985. Fast and sensitive detection of protein and DNA bands by treatment with potassium permanganate. *J. Biochem. Biophys. Methods* **11**:13–20.
- Ballesteros, M. L., C. M. Sánchez, and L. Enjuanes. 1997. Two amino acid changes at the N-terminus of transmissible gastroenteritis coronavirus spike protein result in the loss of enteric tropism. *Virology* **227**:378–388.
- Bass, S. H., M. G. Mulkerin, and J. A. Wells. 1991. A systematic mutational analysis of hormone-binding determinants in the human growth hormone receptor. *Proc. Natl. Acad. Sci. USA* **88**:4498–4502.
- Baudoux, P., C. Carrat, L. Besnardeau, B. Charley, and H. Laude. 1998. Coronavirus pseudoparticles formed with recombinant M and E proteins induce alpha interferon synthesis by leukocytes. *J. Virol.* **72**:8636–8643.
- Brady, J. N., V. D. Winston, and R. A. Consigli. 1997. Dissociation of polyomavirus by the chelation of calcium ions found associated with purified virions. *J. Virol.* **23**:717–724.
- Bremer, A., M. Häner, and U. Aebi. 1998. Negative staining, p. 277–284. *In* J. E. Celis (ed.), *Cell biology. A laboratory handbook*, 2nd ed., vol. 3. Academic Press, San Diego, Calif.
- Brian, D. A., B. G. Hogue, and T. E. Kienzle. 1995. The coronavirus hemagglutinin esterase glycoprotein, p. 165–176. *In* S. G. Siddell (ed.), *The Coronaviridae*. Plenum Press, New York, N.Y.
- Charley, B., and H. Laude. 1988. Induction of alpha interferon by transmissible gastroenteritis coronavirus: role of transmembrane glycoprotein E1. *J. Virol.* **62**:8–10.
- Cheng, R. H., R. J. Kuhn, N. H. Olson, M. G. Rossmann, H. Choi, T. J. Smith, and T. S. Baker. 1995. Nucleocapsid and glycoprotein organization in an enveloped virus. *Cell* **80**:621–630.
- Correa, L., F. Gebauer, M. J. Bullido, C. Suñé, M. F. D. Baay, K. A. Zwaagstra, W. P. A. Posthumus, J. A. Lenstra, and L. Enjuanes. 1990. Localization of antigenic sites of the E2 glycoprotein of transmissible gastroenteritis coronavirus. *J. Gen. Virol.* **71**:271–279.
- Cosson, P. 1996. Direct interaction between the envelope and matrix proteins of HIV-1. *EMBO J.* **15**:5783–5788.
- de Haan, C. A. M., L. Kuo, P. S. Masters, H. Vennema, and P. J. M. Rottier. 1998. Coronavirus particle assembly: primary structure requirements of the membrane protein. *J. Virol.* **72**:6838–6850.
- de Haan, C. A. M., M. Smeets, F. Vernooij, H. Vennema, and P. J. M. Rottier. 1999. Mapping of the coronavirus membrane protein domains involved in interaction with the spike protein. *J. Virol.* **73**:7441–7452.
- Delmas, B., J. Gelfi, R. L'Haridon, L. K. Vogel, O. Norén, and H. Laude. 1992. Aminopeptidase N is a major receptor for the enteropathogenic coronavirus TGEV. *Nature* **357**:417–420.
- Eleouet, J. F., D. Rassaert, P. Lambert, L. Levy, P. Vende, and H. Laude. 1995. Complete sequence (20 kilobases) of the polyprotein-encoding gene 1 of transmissible gastroenteritis virus. *Virology* **206**:817–822.
- Enjuanes, L., D. Brian, D. Cavanagh, K. Holmes, M. M. C. Lai, H. Laude, P. Masters, P. Rottier, S. G. Siddell, W. J. M. Spaan, F. Taguchi, and P. Talbot. 2000. *Coronaviridae*, p. 835–849. *In* M. H. V. van Regenmortel, C. M. Fauquet, D. H. L. Bishop, E. B. Carsten, M. K. Estes, S. M. Lemon, M. A. Mayo, D. J. McGeoch, C. R. Pringle, and R. B. Wickner (ed.), *Virus taxonomy*. Academic Press, New York, N.Y.
- Fischer, F., C. F. Stegen, P. S. Masters, and W. A. Samsonoff. 1998. Analysis of constructed E gene mutants of mouse hepatitis virus confirms a pivotal role for E protein in coronavirus assembly. *J. Virol.* **72**:7885–7894.
- Gajardo, R., P. Vende, D. Poncet, and J. Cohen. 1997. Two proline residues are essential in the calcium-binding activity of rotavirus VP7 outer capsid protein. *J. Virol.* **71**:2211–2216.
- Gebauer, F., W. A. P. Posthumus, I. Correa, C. Suñé, C. M. Sánchez, C. Smerdou, J. A. Lenstra, R. Meloan, and L. Enjuanes. 1991. Residues involved in the formation of the antigenic sites of the S protein of transmissible gastroenteritis coronavirus. *Virology* **183**:225–238.
- Godet, M., R. L'Haridon, J. F. Vautherot, and H. Laude. 1992. TGEV coronavirus ORF4 encodes a membrane protein that is incorporated into virions. *Virology* **188**:666–675.
- Helenius, A., and J. Kartenbeck. 1980. The effects of octylglucoside on the Semliki forest virus membrane. Evidence for a spike-protein-nucleocapsid interaction. *Eur. J. Biochem.* **106**:613–618.
- Homann, H. E., W. Willenbrink, C. J. Buchholz, and W. J. Neubert. 1991. Sendai virus protein-protein interactions studied by a protein-blotting protein-overlay technique: mapping of domains on NP protein required for binding to P protein. *J. Virol.* **65**:1304–1309.
- Jiménez, G., I. Correa, M. P. Melgosa, M. J. Bullido, and L. Enjuanes. 1986. Critical epitopes in transmissible gastroenteritis virus neutralization. *J. Virol.* **60**:131–139.

25. **Laude, H., J. M. Chapsal, J. Gelfi, S. Labiau, and J. Grosclaude.** 1986. Antigenic structure of transmissible gastroenteritis virus. I. Properties of monoclonal antibodies directed against virion proteins. *J. Gen. Virol.* **67**:119–130.
26. **Laude, H., J. Gelfi, L. Lavenant, and B. Charley.** 1992. Single amino acid changes in the viral glycoprotein M affect induction of alpha interferon by the coronavirus transmissible gastroenteritis virus. *J. Virol.* **66**:743–749.
27. **Laude, H., D. Rasschaert, and J. C. Huet.** 1987. Sequence and N-terminal processing of the transmembrane protein E1 of the coronavirus transmissible gastroenteritis virus. *J. Gen. Virol.* **68**:1687–1693.
28. **Laude, H., K. Vanreeth, and M. Pensaert.** 1993. Porcine respiratory coronavirus—molecular features and virus host interactions. *Vet. Res.* **24**:125–150.
29. **Li, M., P. Beard, P. A. Estes, M. K. Lyon, and R. L. Garcea.** 1998. Intercapsomeric disulfide bonds in papillomavirus assembly and disassembly. *J. Virol.* **72**:2160–2167.
30. **Lin, B., and L. A. Heaton.** 1999. Mutational analyses of the putative calcium binding site and hinge of the Turnip Crinkle virus coat protein. *Virology* **259**:34–42.
31. **López, S., J.-S. Yao, R. J. Kuhn, E. G. Strauss, and J. H. Strauss.** 1994. Nucleocapsid-glycoprotein interactions required for assembly of alphaviruses. *J. Virol.* **68**:1316–1323.
32. **Mancini, E. J., M. Clarke, B. E. Gowen, T. Rutten, and S. D. Fuller.** 2000. Cryo-electron microscopy reveals the functional organization of an enveloped virus, Semliki Forest virus. *Mol. Cell* **5**:255–266.
33. **McClurkin, A. W., and J. O. Norman.** 1966. Studies on transmissible gastroenteritis of swine. II. Selected characteristics of a cytopathogenic virus common to five isolates from transmissible gastroenteritis. *Can. J. Comp. Med. Vet. Sci.* **30**:190–198.
34. **Mebatsion, T., F. Weiland, and K.-K. Conzelmann.** 1999. Matrix protein of rabies virus is responsible for the assembly and budding of bullet-shaped particles and interacts with the transmembrane spike glycoprotein G. *J. Virol.* **73**:242–250.
35. **Metsikkö, K., and H. Garoff.** 1990. Oligomers of the cytoplasmic domain of the p62/E2 membrane protein of Semliki Forest virus bind to the nucleocapsid *in vitro*. *J. Virol.* **64**:4678–4683.
36. **Narayanan, K., A. Maeda, J. Maeda, and S. Makino.** 2000. Characterization of the coronavirus M protein and nucleocapsid in infected cells. *J. Virol.* **74**:8127–8134.
37. **Nguyen, V.-P., and B. G. Hogue.** 1997. Protein interactions during coronavirus assembly. *J. Virol.* **71**:9278–9284.
38. **Pogulis, R. J., A. N. Vallejo, and L. R. Pease.** 1996. *In vitro* recombination and mutagenesis by overlap extension PCR, p. 167–176. *In* M. K. Trower (ed.), *In vitro* mutagenesis protocols. Humana Press, Totowa, N.J.
39. **Poisson, F., A. Severac, C. Hourieux, A. Goudeau, and P. Roingeard.** 1997. Both pre-S1 and S domains of hepatitis B virus envelope proteins interact with the core particle. *Virology* **228**:115–120.
40. **Risco, C., I. M. Antón, L. Enjuanes, and J. L. Carrascosa.** 1996. The transmissible gastroenteritis coronavirus contains a spherical core shell consisting of M and N proteins. *J. Virol.* **70**:4773–4777.
41. **Risco, C., I. M. Antón, C. Suñé, A. M. Pedregosa, J. M. Martín-Alonso, F. Parra, J. L. Carrascosa, and L. Enjuanes.** 1995. Membrane protein molecules of transmissible gastroenteritis coronavirus also expose the carboxy-terminal region on the external surface of the virion. *J. Virol.* **69**:5269–5277.
42. **Risco, C., M. Muntión, L. Enjuanes, and J. L. Carrascosa.** 1998. Two types of virus-related particles are found during transmissible gastroenteritis virus morphogenesis. *J. Virol.* **72**:4022–4031.
43. **Salanueva, I. J., J. L. Carrascosa, and C. Risco.** 1999. Structural maturation of the transmissible gastroenteritis coronavirus. *J. Virol.* **73**:7952–7964.
44. **Sánchez, C. M., A. Izeta, J. M. Sánchez-Morgado, S. Alonso, I. Sola, M. Balasch, J. Plana-Durán, and L. Enjuanes.** 1999. Targeted recombination demonstrates that the spike gene of transmissible gastroenteritis coronavirus is a determinant of its enteric tropism and virulence. *J. Virol.* **73**:7607–7618.
45. **Sánchez, C. M., G. Jiménez, M. D. Laviada, I. Correa, C. Suñé, M. J. Bullido, F. Gebauer, C. Smerdou, P. Callebaut, J. M. Escribano, and L. Enjuanes.** 1990. Antigenic homology among coronaviruses related to transmissible gastroenteritis virus. *Virology* **174**:410–417.
46. **Sturman, L. S., K. V. Holmes, and J. Behnke.** 1980. Isolation of coronavirus envelope glycoproteins and interaction with the viral nucleocapsid. *J. Virol.* **33**:449–462.
47. **Vennema, H., G. J. Godeke, J. W. A. Rossen, W. F. Voorhout, M. C. Horzinek, D. J. Opstelten, and P. J. M. Rottier.** 1996. Nucleocapsid-independent assembly of coronavirus-like particles by co-expression of viral envelope protein genes. *EMBO J.* **15**:2020–2028.
48. **Wesley, R. D., R. D. Woods, I. Correa, and L. Enjuanes.** 1988. Lack of protection *in vivo* with neutralizing monoclonal antibodies to transmissible gastroenteritis virus. *Vet. Microbiol.* **18**:197–208.
49. **Woods, R. D., R. D. Wesley, and P. A. Kapke.** 1987. Complement-dependent neutralization of transmissible gastroenteritis virus by monoclonal antibodies. *Adv. Exp. Med. Biol.* **218**:493–500.
50. **Ye, Z., T. Liu, D. P. Offringa, J. McInnis, and R. A. Levandowski.** 1999. Association of influenza virus matrix protein with ribonucleoproteins. *J. Virol.* **73**:7467–7473.